Developments in Using GPS for Oceanographic Remote Sensing: Retrieval of Ocean Surface Wind Speed and Wind Direction

A. Komjathy[1], M. Armatys[1], D. Masters[1], P. Axelrad[1], V.U. Zavorotny[2], and S.J. Katzberg[3]

[1]CCAR/University of Colorado at Boulder, CB 431, Boulder, CO 80309
[2]NOAA/Environmental Technology Laboratory, 325 Broadway, Boulder, CO 80305
[3]NASA Langley Research Center, Code 328, Hampton, VA, 23681-0001

BIOGRAPHIES

Attila Komjathy is currently working on the utilization of GPS reflected signals as a Research Associate at the University of Colorado's Center for Astrodynamics Research. He received his Ph.D. from the Department of Geodesy and Geomatics Engineering of the University of New Brunswick in 1997. His dissertation on the ionospheric total electron content mapping using GPS won the 1998 Canadian Governor General's Gold Medal.

Michael Armatys is a graduate student in the Department of Aerospace Engineering Sciences at the University of Colorado, Boulder. He received his B.S. in Electrical Engineering from Kansas State University in 1996 and his M.S. in Aerospace Engineering from the University of Colorado in 1998. He has worked in the field of GPS applications since 1994 and has been involved with ocean-reflected GPS technology on a NASA GSRP fellowship since 1998.

Dallas Masters is a graduate student in the Department of Aerospace Engineering Sciences at the University of Colorado, Boulder. He received a B.S. in Engineering Science from Trinity University in 1995 and conducted graduate research in satellite remote sensing at Los Alamos National Laboratory until 1998. He has worked in the field of GPS remote sensing since 1998.

Valery Zavorotny is a research scientist at the Environmental Technology Laboratory of the National Oceanic and Atmospheric Administration in Boulder. With a Ph.D., awarded by the (former) USSR Academy of Sciences's Institute of Atmospheric Physics in 1979, he is currently investigating radio wave scattering from rough surfaces and working on novel remote sensing techniques, such as GPS signal scattering from the earth and oceans.

Penina Axelrad is Associate Professor of Aerospace Engineering Sciences at the University of Colorado, Boulder. Her research is focused on GPS technology and data analysis for aerospace applications. She has been involved in GPS-related research since 1985, previously at Stanford University and Stanford Telecommunication, Inc.

Stephen Katzberg has been a research scientist with NASA Langley Research Center since 1966. He holds a B.S.EE. degree from MIT, and M.S.EE. and Ph.D. degrees from the University of Virginia. He is among those who pioneered the research of GPS surface reflected signals for various remote sensing applications. He holds several patents and published extensively on the subject.

ABSTRACT

Global Positioning System (GPS) signals reflected from the ocean surface have potential use for various remote sensing purposes. Some possibilities are measurements of surface roughness characteristics from which wave height, wind speed and direction could be determined. In this paper, recent reflected GPS measurements collected via aircraft with a delay mapping GPS receiver, are used to explore the possibility of determining ocean surface wind speed and direction during Hurricanes Michael and Keith in October, 2000. To interpret the GPS data, a theoretical model is used to describe the correlation power of the reflected GPS signals for different time delays as a function of geometrical and environmental parameters. Wind direction estimates are based on a multiple satellite non-linear least squares solution. The estimated wind speed using surface-reflected GPS data collected at a variety of wind speed conditions shows an overall agreement better than 2 m/s with data obtained from

Presented at the ION 2001 National Technical Meeting, Long Beach, CA, January 22-24

nearby buoy data and independent wind speed measurements derived from TOPEX/Poseidon, ERS, and QuikSCAT observations. Wind direction agreement with QuikSCAT measurements appear to be at the 30 degree level. In addition to the actual results we also present an error analysis describing the expected performance of the GPS technique.

INTRODUCTION

The use of GPS as a forwardscatter remote sensing tool has come to fruition in the last few years (Katzberg [1996], Garrison et al. [1997, 1998, 1999], Komjathy et al. [1998, 1999], Lin et al. [1999], Armatys [2000]). NASA researchers Stephen J. Katzberg of LaRC and James L. Garrison now at Purdue University have determined the properties of the ocean-reflected signal and have developed a specialized GPS receiver called the Delay-Mapping Receiver (DMR) to measure the reflected signals [Garrison et al., 1997].

Other investigations of ocean reflected GPS signals are being conducted by the Jet Propulsion Laboratory (JPL) and the European Space Agency (ESA), focused primarily on the application of reflected GPS signal tracking to altimetry [Martin-Neira, 1993]. These groups have conducted a number of experiments from static locations and aircraft, and investigated signals received from a spaceborne antenna [Lowe et al., 2000a, 2000b].

Using the DMR and models to predict the interaction of the L1 GPS signal at 1575.42 MHz, researchers at NASA Langley Research Center, Purdue University and the University of Colorado at Boulder have been able to estimate wind speeds on the ocean surface with an accuracy of about 2 m/s. Results to date have advanced the understanding of reflected GPS signals and provided direct experimental evidence of their application to ocean remote sensing and mapping.

The model employed in this paper's estimation process was developed by Zavorotny and Voronovich (Z-V) and is documented extensively in Clifford et al. [1998], Zavorotny and Voronovich [2000] and Komjathy et al. [2000]. The Z-V model employs a forwardscatter radar equation with the geometric optics limit of the Kirchhoff Approximation. For backscattering theory and applications, the interested reader is referred to Ulaby et al. [1986]. The wave spectra used by the Z-V model is that from Elfouhaily et al. [1997].

The Z-V model takes the form:

$$\left\langle \left|Y(\tau, f_c)\right|^2 \right\rangle = T_i^2 \int \frac{\left|\Re\right|^2 D^2(\vec{\rho})\,\Lambda^2[\tau - (R_0 + R)/c]}{4\pi\, R_0^2(\vec{\rho})\, R^2(\vec{\rho})\, q_z^4} \times \left|S[f_D(\rho) - f_c]\right|^2 P\left(-\frac{\vec{q}_\perp}{q_z}\right) q^4\, d^2\rho \,. \quad (1)$$

where $\left\langle \left|Y(\tau, f_c)\right|^2 \right\rangle$ is the reflected power for any delay bin τ and Doppler offset f_c; T_i is the integration time in seconds; $\Re$ is the complex reflectivity of the ocean at L1; D is the antenna gain; Λ is the correlation function of the GPS C/A code; S is the Doppler sync function; P is the probability density function (PDF) of the surface slopes; q is the magnitude of the scattering vector $\vec{q}$; R_0 is the distance from some point on the surface point to the GPS satellite; R is the distance from the GPS receiver to some point on the surface; c is the speed of light; f_D is the Doppler shift at the specular point; f_c is the compensation frequency or the Doppler offset to some point $\vec{\rho}$; and $\vec{\rho}$ is a vector from the specular point to some other point on the surface. For our aircraft experiments discussed in this paper, equation (1) can be simplified and S set to unity.

INSTRUMENT AND DATA

The use of GPS in a bistatic radar configuration to measure surface properties relies upon our ability to extract information from the reflected signal. For standard GPS navigation applications, the receiver's main functions are to measure the signal delay from the satellite (the pseudorange measurement) and the rate of change of the range (the Doppler measurement) (see e.g., Parkinson et al. [1996]). Conversely, in our remote sensing application, the primary measurement is the received power from a reflected signal for a variety of delays and Doppler values. The basis of this measurement and its sensitivity to the surface conditions is discussed in the following paragraphs.

The Delay Mapping Receiver (DMR) is a software configurable GEC Plessey (now Mitel Semiconductor) GPS Builder-2 receiver modified to observe reflected LHCP signals from two GPS satellites and to record correlator power at 10 consecutive half-chip intervals. The half-chip intervals are analogous to range bins in a radar receiver and are used to isolate power reflecting from a specific region on the ocean surface. Signals reflected from the ocean surface originate from a glistening zone (see Figure 1a) surrounding a nominal specular reflection point. The size and shape of the glistening zone are functions of the roughness of the ocean surface. To measure the reflected power from this glistening zone, the receiver-generated pseudorandom noise codes are delayed in time with respect to directly received, line-of-sight signals. This isolates power originating from the region

surrounding the specular reflection point. The shape of the resulting waveform of power-versus-delay is dependent upon the roughness of the ocean surface (see Figure 1b). This roughness is in turn a function of the surface wind speed and direction, and therefore provides a means to retrieve these geophysical parameters from the GPS reflected signal power measurement.

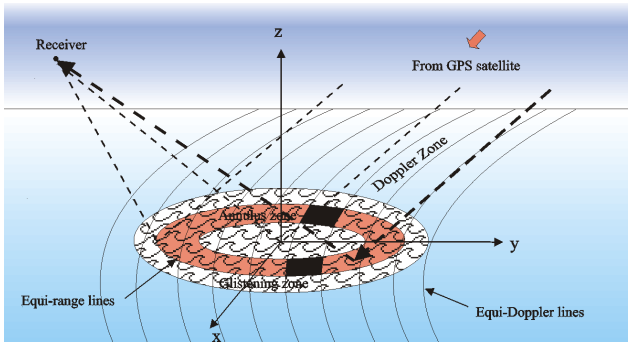

Figure 1a. Illustration for ocean-reflected GPS signals.

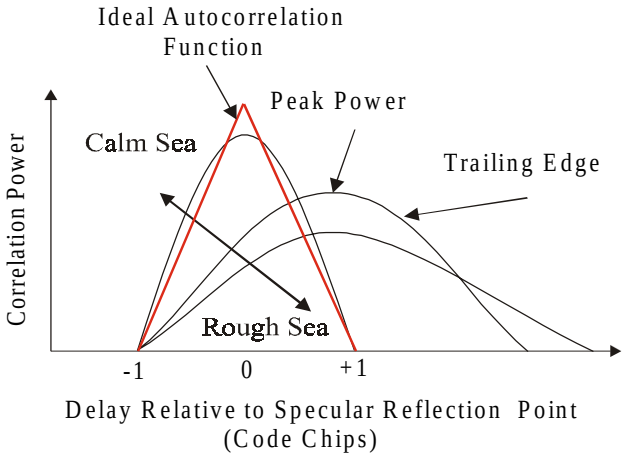

Figure 1b. Correlation function shapes for ideal direct GPS signal and for reflected signals from rough surfaces.

METHOD FOR WIND SPEED AND WIND DIRECTION RETRIEVAL

Preprocessing the Data. Before the estimator can make use of the reflected GPS data, they must be preprocessed. Preprocessing takes place in several steps. First, the noise floor is computed for each data set. This is done by computing the mean of all the points before the first correlation peak of the reflected signal. After computing the noise floor, it is subtracted from all data points. These reflected data points are then normalized by dividing by the total reflected power. Normalization is necessary to remove effects of uncalibrated receiver gains. The total reflected power is computed by summing all of the correlation measurements for one waveform, essentially integrating the correlation waveform. Total reflected power is chosen for normalization because it should be nearly constant due to conservation of energy. Finally, the data is broken into one-minute segments for use by the estimator.

An estimate of the path delay, τ, is computed using post-processed positions of the satellite and receiver. The satellite positions are interpolated from International GPS Service's (IGS) 15-minute precise positions, and the receiver positions are interpolated using the receiver's navigation solution. Using these positions and the WGS-84 ellipsoid, an estimate of the specular reflecting point coordinates on the earth surface is computed. The path delay is then estimated from these three positions. Because the delay variable computed from the receiver and satellite geometry with respect to the WGS-84 ellipsoid may contain errors, a shifting parameter is introduced. A scaling parameter is also introduced which compensates for errors in the assumptions made during normalization of the measured power. Because the total power measured over the 10 delay bins fails to include power over the same range of delay as the modeled waveform, inclusion of a scale factor accounts for this discrepancy during normalization. During preprocessing, we also quality-check the data and eliminate outliers by computing the mean and standard deviation of the reflected power in each delay bin.

Main Processor. The state for the estimation process contains wind speed, wind direction and as an option, path delay error estimates, and scaling parameters can also be simultaneously estimated. For routine data processing, the software is able to estimate path delay errors by aligning the waveform leading edges.

The basis for wind direction determination is that the PDF of surface slopes is wider in the direction of the wind. This produces an asymmetry in the glistening zone. With delay measurements from a single satellite, it is not possible to unambiguously identify this asymmetry direction because the integration over a delay bin or annulus tends to obscure the uneven distribution, creating an ambiguity with respect to the asymmetry direction. Recovery is possible with multiple satellites under the condition that the glistening zones are due to the same surface wind conditions. Because the annuli for the two or more satellites are not mutually concentric, these measurements provide the necessary conditions for observing the PDF asymmetry.

In the latest version of our algorithm, we implemented the option to process any number of satellites in a single batch to fit the measured to the modeled waveforms using a non-

linear least squares algorithm in MATLAB. In the algorithm, residuals are minimized using a Nelder-Mean direct search method to adjust the state.

By processing two or three satellites simultaneously, both wind speed and direction can be solved. To make the multiple satellite estimator code run faster, we created an extensive waveform database using combinations of receiver height, elevation angle, wind speeds and wind directions.

FLIGHTS

The NOAA Hurricane Research Division, with the assistance of NOAA/Environmental Technology Laboratory, installed a DMR GPS receiver in one of the WP-3D Hurricane Hunters N42RF "Kermit". Members of NOAA Airborne Operations Center at MacDill AFB installed the receiver in August 2000. The first data was collected from the outer edges of Hurricane Keith on October 1, 2000. The emergence of Hurricane Michael presented the first opportunity to traverse the core of a tropical cyclone on October 18, 2000. Hurricane Michael formed in the Western Atlantic the evening of October 16. It reached tropical storm strength the next morning and was classified a hurricane that same afternoon. Michael increased forward speed the night of October 18. It sped northward, made landfall in Newfoundland, Canada on October 19, and quickly began losing tropical characteristics. At the time of the aircraft penetration, the storm was moving at approximately 18 m/s. Figure 2 is a map derived from the GPS position information, which shows the aircraft flight path from MacDill, Florida into the center of Hurricane Michael and subsequent flying in and around storm. The cross represents the center of the storm (from Hurricane Research Division data) during the time the GPS surface reflection data was taken. Preliminary results and findings of the data processing were presented in Katzberg [2001].

For comparison purposes, we used wind speeds from TOPEX/Poseidon dual-frequency altimeter, ERS altimeter, buoy measurements, flight level wind speed and on-board step-frequency microwave radiometer (SFMR) data (see e.g., Ulaby et al. [1986]). To compare GPS-derived wind direction with an independent ground-truth we used QuikSCAT-derived wind measurement. For detailed discussion of different satellite wind speed retrieval techniques, see Stewart [1985].

RESULTS

Wind Speed Retrieval. The aircraft flew out from the coast at an altitude of 4500 meters. It descended to 1400 meters traversed the eye of the storm and then descended further

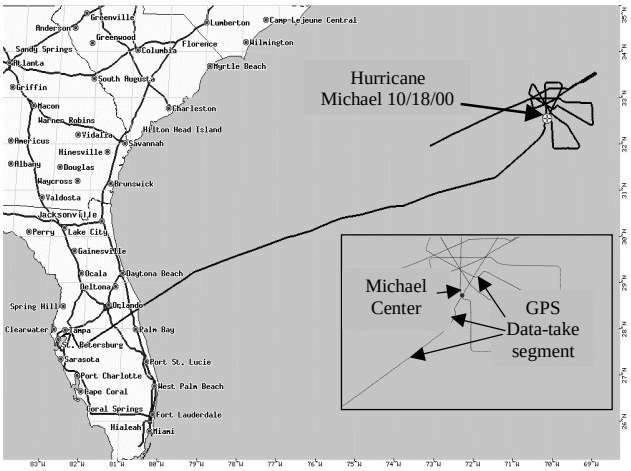

Figure 2. Flight trajectory for Hurricane Michael of October 18, 2000 adapted from Katzberg [2001].

to 500 meters where it stayed for the bulk of the time the GPS equipment was operated. At approximately 15:50 UT, the aircraft flight path crossed a TOPEX ground track. Figure 3 shows the GPS-derived wind estimates at this time, for each satellite separately. A combined solution using PRNs 15, 21 and 23 is presented in Figure 4. In Figure 3, we also plotted the mean of the individual solutions along with the standard deviations. The estimated wind speed estimates using single satellites ranges between 6 m/s and 10 m/s. The combined solution in Figure 4, agrees with the TOPEX solution within an RMS of 0.7 m/s. The RMS of the individual satellite estimates is 1.2 m/s.

At approximately 14:55 UT, the aircraft crossed the ERS ground track. We again processed the satellites separately as shown in Figure 5 along with the mean and standard deviation. A combined solution was obtained showing better agreement with the corresponding ERS ground-truth (0.7 m/s RMS, see Figure 6) than the average solution from individual satellites (0.9 m/s RMS). We believe that the larger differences near the start of the graph are the result of a larger separation between the aircraft position and the ERS ground track at that point.

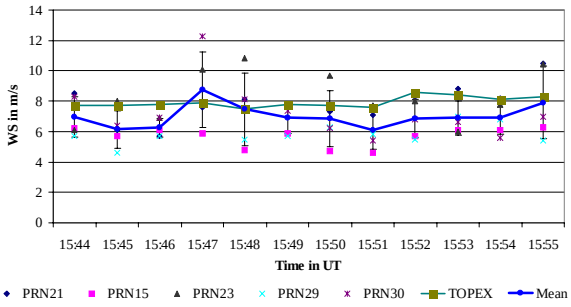

Figure 3. Satellite by satellite GPS wind speed (WS) solution for TOPEX pass.

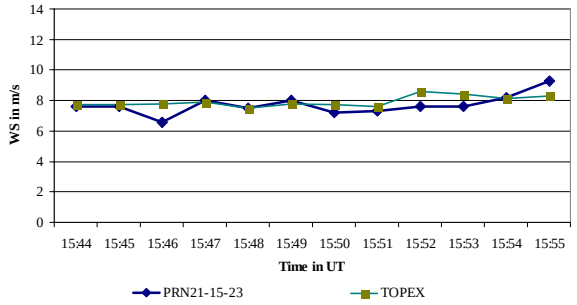

Figure 4. Multiple satellite GPS wind speed (WS) solution for TOPEX pass.

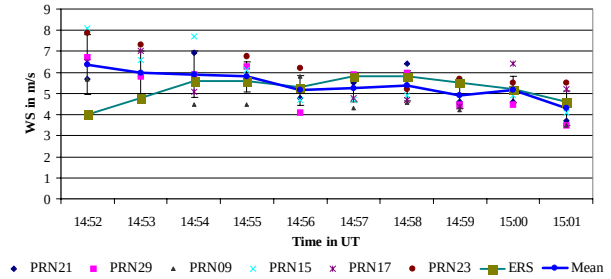

Figure 5. Satellite by satellite GPS wind speed (WS) solution for ERS pass.

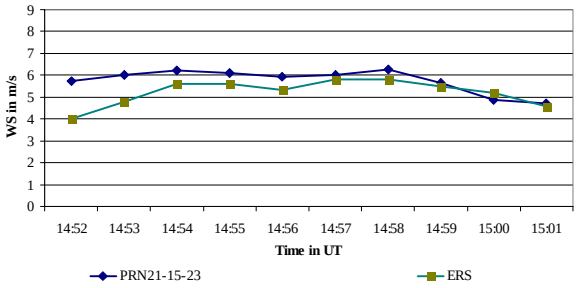

Figure 6. Muliple satellite GPS wind speed (WS) solution for ERS pass.

In Figure 7, we show the combined solution for a three-hour segment of the flight track that also included the TOPEX and ERS data segments. Also displayed is the aircraft altitude. Time tags corresponding to TOPEX and ERS passes, and buoy measurements are superimposed showing generally a good agreement between GPS wind estimates and ground-truth for the pre-hurricane part of the flight. Furthermore, data from Hurricane Research Division of NOAA representing "flight level wind speed" (FLWS) was obtained and plotted in Figure 7. FLWS data was provided in 1-minute and 10-second time series. In Figure 7, due to similarities between the two time series, we only plotted the 1-minute averaged data set. FLWS data is derived from the drift the aircraft experiences when flying into the storm. Also displayed is the time series from step-frequency microwave radiometer (SFMR). At approximately 16:30 UT, the aircraft was approaching the hurricane region. This is apparent in rapid increases in the wind speed from both FLWS and SFMR data. At around 16:55 UT, the aircraft flew over the eye of the hurricane. The high variability of the GPS-retrieved wind speed made the comparison difficult. The peak GPS wind speeds seem to be consistent with the SFMR data, but capturing the eye of the hurricane was unsuccessful. It is possible that this is because the rapid movement of the storm did not allow for the condition of fully developed seas assumed in the wave spectrum and Z-V models. Furthermore, the aircraft descending from 4500 to 1400 meter altitude made waveforms become sharp and narrow resulting in the modeling and retrieval process more likely to fail.

In Figure 8, we show an example for 15:44 UT (see Figures 3 and 4) of the estimator convergence in terms of both the wind speed estimate and the sum of the squared measurement residuals. The filter was initialized with a wind speed of 10 m/s and scaling parameter set to unity. It is shown that after approximately 70 iterations, the wind speed converges to 7.8 m/s. In most cases, convergence is reached in fewer than 30 iterations when the state estimates are initialized with the solution from the previous segment wind speed estimate.

Wind Direction Retrieval. The second data set we present is for October 1, 2000, taken from the outer edges of Hurricane Keith in the Gulf of Mexico to the west of Florida. Wind speeds ranged from 6 m/s to 10 m/s. What distinguishes this data set from Michael is the fact that we have QuikSCAT wind field data available that was taken within one hour of the GPS measurements. In this case, we retrieved wind speed as well as wind direction information using the multiple satellite solution from PRNs 01, 03 and 13 as described earlier.

In Figure 9, we plot the GPS-derived wind speed and direction solution superimposed on the QuikSCAT wind field plot. The aircraft was flying from west to east direction. Wind speeds are plotted next to the base of the arrows representing the GPS-estimated wind directions. The left part of the flight track shows a good agreement in both wind speeds and wind directions.

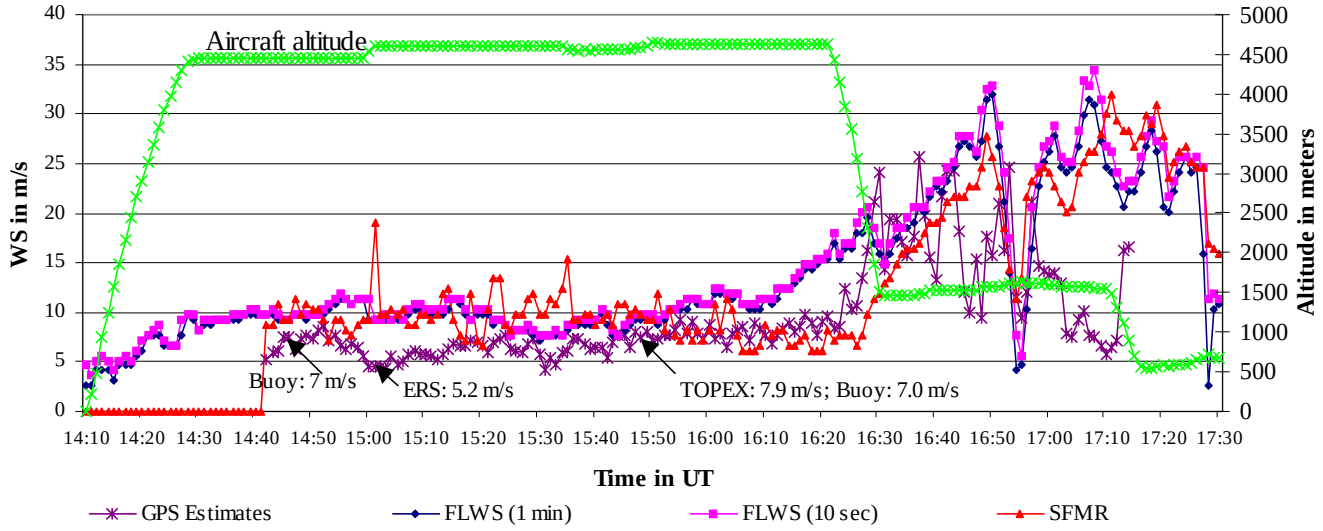

Figure 7. GPS wind speed (WS) estimates along the flight path for Hurricane Michael of October 18, 2000.

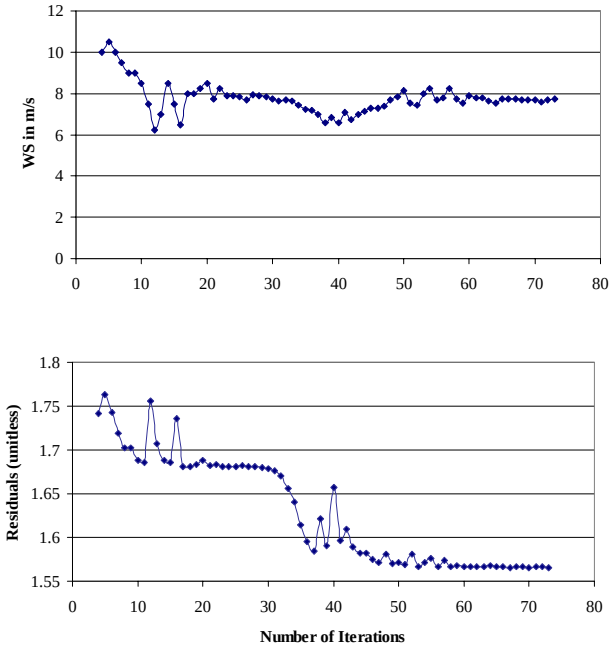

Figure 8. An example of wind speed (WS) convergence showing dependence between number of iterations, estimated wind speed and residuals for the TOPEX pass.

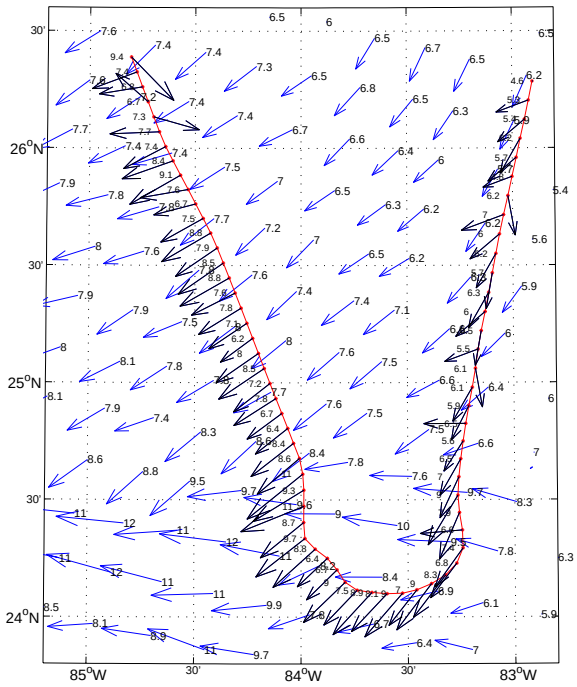

Figure 9. GPS-derived wind vector estimates for the vicinity of Hurricane Keith of October 1, overlaid on QuikSCAT wind field measurements.

The flight path on the right hand side indicates fluctuating wind direction with stable wind speeds. We believe that the reason for the unstable wind direction estimates is rapidly changing aircraft altitude as it was getting closer to the Florida coast. The first few GPS wind direction estimates also show some fluctuations even though the wind speeds are consistent with QuikSCAT data. The discrepancy in wind direction might be due to the fact that our estimator flagged too many data points as outliers resulting in smaller number of waveforms to be available to the estimator.

It is interesting to see that GPS-derived wind is mostly in south-west direction, whereas QuikSCAT data shows similar wind direction only above 24°30'. Below this latitude QuikSCAT wind is predominantly westerly. One possible explanation is that our bistatic GPS scattering model assumes well developed seas. This simplifying assumption could limit our accuracy in this coastal region where the Cuban land mass is approximately 50 km to the south. Furthermore, ocean currents typical for the Cuban coastal region, not taken into account in our model, may also have an impact on our GPS-derived wind field. The

fact that we have good agreement with QuikSCAT in well developed sea conditions points us to the need for further studying the effect of un-developed seas conditions.

In Figure 10, we plotted an example for estimated wind speed, wind direction and residuals to demonstrate the convergence of the solution on the accepted truth. It is shown that after 40 iterations the solution converges on 7.6 m/s wind speed and about 30 degree wind direction. QuikSCAT indicates 7.6 to 7.8 m/s wind speed and about 40 degrees wind direction.

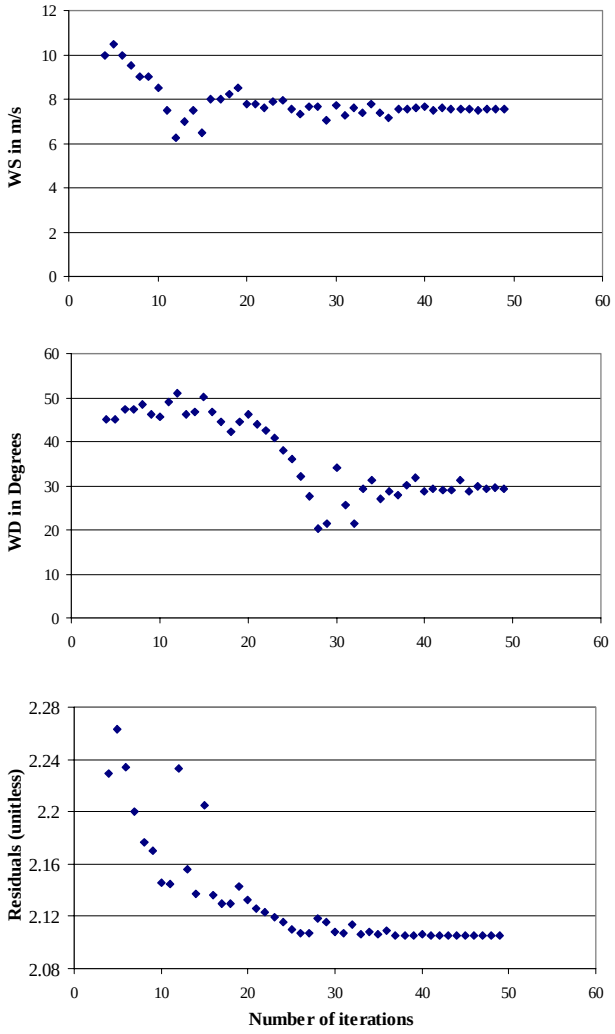

Figure 10. An example for wind speed (WS) and wind direction (WD) convergence for October 1, 2000.

ERROR ANALYSIS

In this section, we investigate the non-linear wind speed and wind direction estimator convergence properties. In Figures 11 and 12, we computed the combined solution residuals using all possible combinations of wind speed (1 m/s increments) and wind directions (10 degree increments). In Figure 11, it is shown that the minimum of the residuals occurs for wind speeds between 6 and 8 m/s. On the other hand, in Figure 12, we show that the minimum of the residuals are obtained for wind direction between 20 and 40 degrees. The individual curves represent a solution with different wind speeds between 3 and 15 m/s starting with 3 m/s at the top. We can clearly see that the difference between measured and modeled values (the residuals) are at the minimum when the right answer (WS and WD) is used to compute the measurement residuals. In Figure 12, we can realize that in the vicinity of the QuikSCAT result, (7 or 8 m/s) there exist solutions with combinations of wind speeds and wind directions resulting in the same sum of the squared residuals. To demonstrate this, we plotted the residuals using the combinations of wind speeds and wind directions. In Figure 13, iso-residual lines show possible combinations of wind speeds and wind directions resulting in the same minimum of the sum of the squared residuals. The “hole” in the middle shows a set of solutions close to the final solution. However, the estimator indicates that the sum of the squared residuals are at the minimum at the middle of the “hole” that can be characterized with wind speed of 7.6 m/s and wind direction of 30 degrees which is in very good agreement with the QuikSCAT measurements.

A reliable wind direction estimate cannot be obtained using delay measurements from a single satellite. This is demonstrated in Figure 14. Although the estimated wind speed is about 8 m/s, the wind direction is estimated to be near 140 degrees, coinciding with the incidence angle of the satellite with an additional ambiguity at about 20 degrees. There are two types of ambiguities in the GPS wind direction retrieval. Firstly, there is a 180 degree ambiguity, related to the symmetry of the PDF of slope in up/down wind direction. This ambiguity cannot be resolved even using multiple satellites. Secondly, there is the ambiguity related to the symmetry with respect to the incidence plane. Indeed, there are two possible angles between the incidence plane and wind direction that create the same GPS reflected signal power. Therefore, the ambiguity can only be solved for using additional simultaneously observed satellites. In Figure 15, we plotted the map of wind speeds and wind directions using one satellite only. The estimator shows a larger pool of possible solutions before finally arriving at 8 m/s wind speed and 170 degree wind direction (aligned with the incident plane).

We also computed the repeatibility of the solutions based upon consecutive and independent 1-minute data segments with the same three satellites. We assume that the wind speed and wind direction do not change over a 10-minute window. Computing the repeatibility gives a measure of the effect of measurement noise on the actual

solution. This analysis shows that over a 10-minute arc, the standard deviations of the wind speed and direction are 0.7 m/s and 9 degrees, respectively. As to the accuracy of our GPS-derived wind direction estimates, the processed data using the combined solution indicated a better than 30 degree agreement with the QuikSCAT measurement. This is encouraging since the overall reported QuikSCAT wind direction accuracy is about 20 degrees.

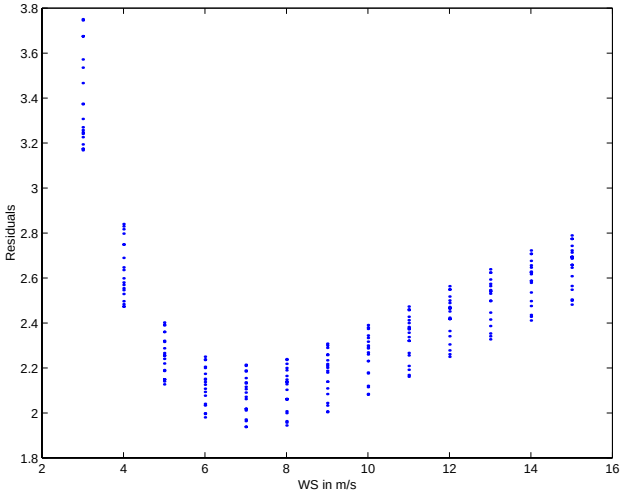

Figure 11. Residuals (unitless) versus wind speed (WS) for October 1 data set.

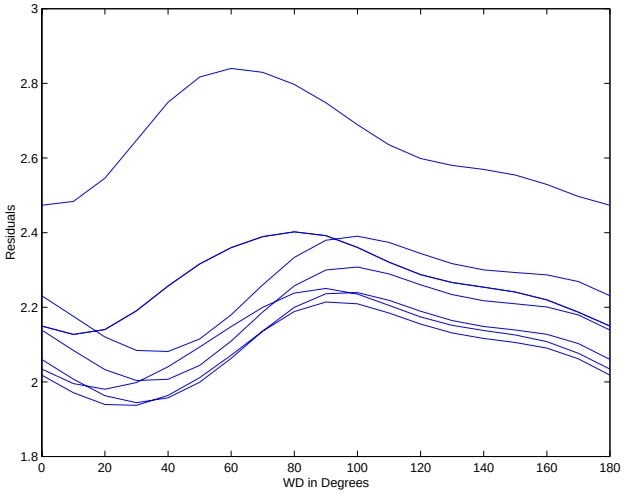

Figure 12. Residuals (unitless) versus wind direction (WD) for October 1 data set.

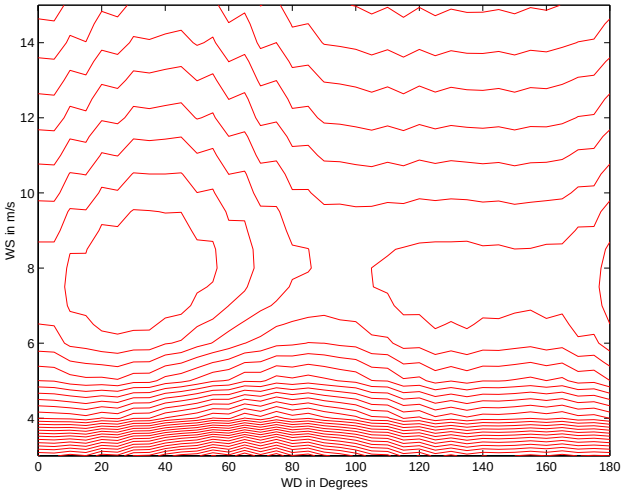

Figure 13. Wind direction (WD), wind speed (WS) and residuals map for the combined multi-satellite solution.

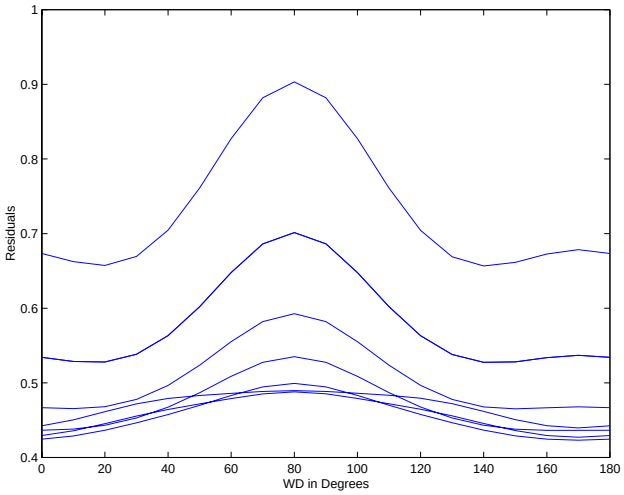

Figure 14. Illustration of unreliable WD estimation using a single satellite (PRN03).

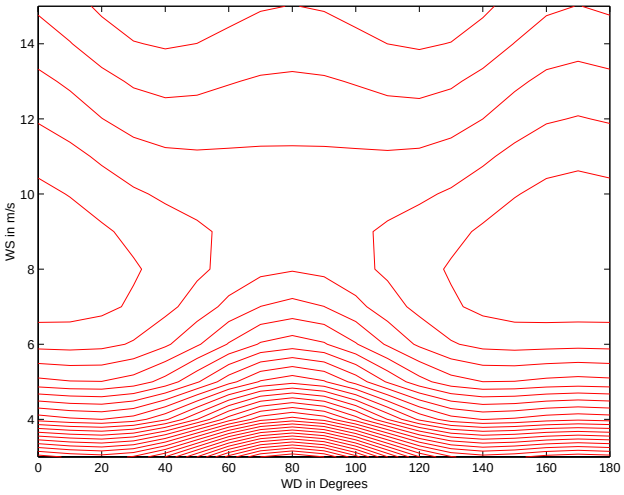

Figure 15. Wind direction (WD), wind speed (WS) and residuals map using a single satellite PRN03.

CONCLUSIONS AND FUTURE RESEARCH

We have demonstrated wind speed and wind direction retrievals using a novel multi-satellite approach combined with non-linear least squares estimation. GPS-derived wind speed and wind direction is compared wind TOPEX, ERS, buoy and QuikSCAT measurements. We found that processing surface reflected GPS signals in a combined solution, as opposed to a satellite by satellite solution, gives us better wind speed agreement, at the level of 2 m/s, with other independent techniques for a variety of wind speed conditions ranging from 3 to 10 m/s. A comparison between GPS-derived wind direction and QuikSCAT wind field showed a better than 30 degree agreement in wind direction. We also demonstrated that it is not possible to estimate wind direction with delay measurements from a single satellite.

Future research will investigate the performance of the technique during high (> 15 m/s) wind conditions and in coastal regions. Additional model enhancements to account for more variable conditions and improvements to data quality and processing are required to achieve progress in these more challenging conditions.

ACKNOWLEDGMENTS

This research has been sponsored at the University of Colorado by a grant from NASA HQ (NAG5-9727), and at NOAA/ETL by RTOP 622-47-55. We appreciated the assistance of Dr. Peter Black of NOAA Hurricane Research Center in providing us with the wind speed data.

REFERENCES

Armatys, M., D. Masters, A. Komjathy, P. Axelrad, and J.L. Garrison (2000). "Exploiting GPS as a New Oceanographic Remote Sensing Tool." On the CD-ROM of *Proceedings of the ION National Technical Meeting*, Anaheim, CA, 26-28 January 2000.

Clifford S.F., V.I. Tatarskii, A.G. Voronovich, and V.U. Zavorotny (1998). "GPS Sounding of Ocean Surface Waves: Theoretical Assessment." In the *Proceedings of IEEE International Geoscience and Remote Sensing Symposium: Sensing and Managing the Environment*, Piscataway, NJ, pp. 2005-2007.

Elfouhaily, T., Chapron, B., Katsaros, K., and Vandemark, D. (1997). "A Unified Directional Spectrum for Long and Short Wind-driven Waves," *Journal of Geophysical Research*, Vol. 102, pp. 15,781-15,796, 1997.

Garrison, J.L., Katzberg, S.J., and Howell, C.T. (1997). "Detection of ocean reflected GPS signals: Theory and experiment." In the *Proceedings of the IEEE Southeastcon*, Blacksburg, 12-14 April, pp. 290-294.

Garrison, J.L., Katzberg, S.J. and Hill, M.I. (1998). "Effect of Sea Roughness on Bistatically Scattered range Coded Signals from the Global Positioning System." *Geophysical Research Letters*, 25:2257-2260.

Garrison, J.L., A. Komjathy, V. Zavorotny, and S.J. Katzberg (1999). "Wind Speed Measurement from Bistatically Scattered Signals." *IEEE Transactions on Geoscience and Remote Sensing* (in review).

Katzberg, S. J. and Garrison, J.L. (1996). "Utilizing GPS to Determine Ionospheric Delay over the Ocean." NASA TM 4750, December.

Katzberg, S.J., R.A. Walker, J.H. Roles, T. Lynch, and P.G. Black (2001). "First GPS Signals Reflected from the Interior of a tropical storm: Preliminary Results from Hurricane Michael." Submitted to the *Geophysical Research Letters*.

Komjathy, A., V.U. Zavorotny, J.L. Garrison (1999). "GPS: A New Tool for Ocean Science." *GPS World*, Vol. 10, No. 4, pp. 50-56.

Komjathy, A., V. U. Zavorotny, P. Axelrad, G.H. Born, and J. Garrison (2000). "GPS Signal Scattering from Sea Surface: Comparison between Experimental Data and Theoretical Model." *Remote Sensing of Environment*, Vol. 73, pp. 162-174.

Lin, B., Katzberg, S.J., Garrison, J.L., and Wielicki, B.A.,(1999). "The relationship between the GPS signals reflected from sea surface and the surface winds: modeling results and comparisons with aircraft measurements." *Journal of Geophysical Research*, Vol. 104(C9), pp. 20713-20727.

Lowe, S.T., C. Zuffada, J.L. LaBrecque, M. Lough, J. Lerma, and L.E. Young (2000a). "An Ocean-Altimetry Measurement Using Reflected GPS Signals Observed From a Low-Altitude Aircraft." On the CD-ROM of the *Proceedings of IEEE International Geoscience and Remote Sensing Symposium (IGARSS)*, Honolulu, HI, July 24-28.

Lowe, S.T., J.L. LaBrecque, C. Zuffada, L.J. Romans, L.E. Young, and G.A. Hajj. (2000b). "First Airborne Observation of Earth-Reflected GPS Signal." Submitted to *Radio Science*.

Martin-Neira, M. (1993). "A Passive Reflectometry and Interferometry System (PARIS) Application to Ocean Altimetry." *ESA Journal*, Vol. 17, pp. 331-355.

Parkinson, B.W., J.J. Spilker, P. Axelrad, and P. Enge (eds.) (1996). *Global Positioning System: Theory and Applications*, Vol. I & II, American Institute of Aeronautics and Astronautics, Washington, DC.

Stewart, R.H. (1985). *Methods of Satellite Oceanography*, University of California Press, Berkeley, CA.

Ulaby, F.T., Moore, R.K. and Fung, A.K. (1986). *Microwave Remote Sensing, Active and Passive*, Artech House.

Zavorotny, V. U. and Voronovich (2000). "Scattering of GPS signals from the ocean with wind remote sensing application." *IEEE Transactions in Geoscience and Remote Sensing*, Vol. 38, No. 2, pp. 951-964.